

Splitting of the Fermi point of strongly interacting electrons in one dimension: A nonlinear effect of spin-charge separation

O. Tsyplatyev

Institut für Theoretische Physik, Universität Frankfurt, Max-von-Laue Straße 1, 60438 Frankfurt, Germany



(Received 3 January 2022; revised 21 February 2022; accepted 1 March 2022; published 22 March 2022)

A system of one-dimensional electrons interacting via a short-range potential described by Hubbard model is considered in the regime of strong coupling using the Bethe ansatz approach. We study its momentum distribution function at zero temperature and find one additional singularity at the $3k_F$ point. We identify that the second singularity is of the same Luttinger liquid type as the low-energy one at k_F . By calculating the spectral function simultaneously, we show that the second Luttinger liquid at $3k_F$ is formed by charge modes only, unlike the known one around k_F consisting of both spin and charge modes. This result reveals the ability of the spin-charge separation effect to split the Fermi point of free electrons into two, demonstrating its robustness beyond the low-energy limit of Luttinger liquid where it was originally found.

DOI: [10.1103/PhysRevB.105.L121112](https://doi.org/10.1103/PhysRevB.105.L121112)

Interactions have a dramatic effect on electrons in one dimension (1D) that has been attracting a significant interest in condensed-matter physics for a long time [1]. Their low-energy excitations become quantized density waves described by the Tomonaga-Luttinger liquid (TLL) theory based on linearization of the spectrum around the Fermi points [2–4]. A hallmark prediction of this theory is separation of the spin and charge degrees of freedom of the underlying electrons into density waves of two distinct types with different velocities [4,5]. Two linear dispersions originating from the Fermi point were observed in experiments on magnetotunneling spectroscopy in semiconductors [6,7], on photoemission in organic [8] and strongly anisotropic [9] crystals, and on time-resolved microscopy in cold atoms [10], establishing firmly this phenomenon.

More recently, the theoretical interest was focused on spectral nonlinearity since it breaks construction of the TLL theory altogether [11] but, on the other hand, is unavoidable at any finite distance from the Fermi energy in a Fermi system. The Boltzmann equation approach to weakly interacting Fermi gas predicts a finite relaxation time due to nonlinearity [12–14], suggesting decay of the many-body modes. Application of the mobile impurity model to Luttinger liquids predicts survival of spin-charge separation, at least, in a weak sense as a singularity—consisting of a mixture of spin and charge modes—at the spectral edge with nonlinear dispersion [15–17]. At the same time, the continuing experimental progress is starting to provide information on effects beyond the low-energy regime [18–22]. In one of these experiments [22], the spin-charge separated modes at low energy were observed to extend to the whole conduction band forming a pair of parabolic dispersions characterized by two incommensurate masses, raising the question if the spin-charge separation phenomenon manifests itself directly in other properties of the whole Fermi sea.

We explore such a possibility theoretically in this Letter by studying the momentum distribution function for a Fermi system with short-range interactions described by the Hubbard model in which the spin-charge separation is well established in the TLL limit [1]. Using the microscopic methods of the

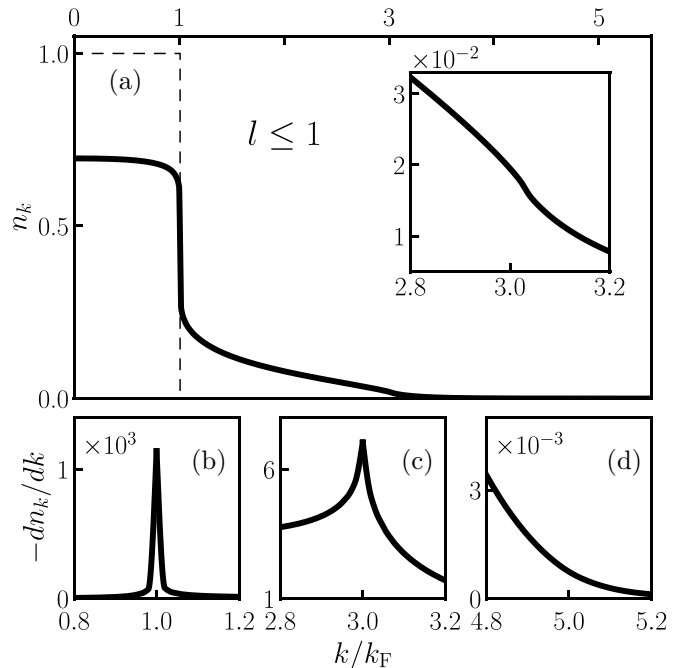


FIG. 1. (a) Momentum distribution function n_k in the ground state of the model in Eq. (1) evaluated in the $U/t = \infty$ limit using Eqs. (6)–(9), and (11) where the two leading levels of the hierarchy of modes $l \leq 1$ were taken into account in the sum in Eq. (11) for $N = 200$ particles (solid line) and for free particles $U/t = 0$ (dashed line). The inset: Zoom in around $3k_F$. (b)–(d) First derivative dn_k/dk around the k_F , $3k_F$, and $5k_F$ points, respectively.

Bethe ansatz in the strong-coupling limit ($U = \infty$) not restricted to low energy [23], we find (at $T = 0$) one extra divergence at $3k_F$ in addition to the usual Fermi point at k_F , see Fig. 1. Both singularities are of the same order in the first derivative dn_k/dk , revealing the ability of spin-charge separation to split one Fermi point of free electrons into two [24]. It is a direct manifestation of this phenomenon in the whole Fermi sea, far away from the TLL limit. Around the second point, we find a power-law behavior of n_k , $n_k \sim \dots + \text{sgn}(k - 3k_F)|k - 3k_F|^{\alpha_{3k_F}}$ with a real exponent of the TLL type $\alpha_{3k_F} = 0.787 \pm 0.067$. However, this exponent does not correspond to the known exponents for spinful or spinless TLLs at k_F [1]. By calculating simultaneously the spectral function we show that, out of the spin-charge separated linear modes around k_F , only the charge branch extends through the nonlinear region to form a TLL around $3k_F$, identifying it as a TLL of a new kind.

We analyze fermions with spin-1/2 interacting via a short-range potential that are described by the 1D Hubbard model,

$$H = -t \sum_{j,\alpha} (c_{j\alpha}^\dagger c_{j+1,\alpha} + c_{j\alpha}^\dagger c_{j-1,\alpha}) + U \sum_j n_{j\uparrow} n_{j\downarrow}, \quad (1)$$

where $c_{j\alpha}$ are the Fermi operators at site j , α is the spin-1/2 index \uparrow or \downarrow , $n_{j\alpha} = c_{j\alpha}^\dagger c_{j\alpha}$ is the local density operator of the spin species α , t is the hopping amplitude describing the kinetic energy, and $U > 0$ is the repulsive two-body interaction energy. Below, we consider the periodic boundary conditions $c_{j+L} = c_j$ for a 1D lattice consisting of L sites and for N -particle states we impose the constraint of low particle density $N/L \ll 1$ [25]. In the strong-interaction limit $U/t = \infty$, the spectrum of the model in Eq. (1) is given by the following Lieb-Wu equations [26,27],

$$Lk_j - P_s = 2\pi I_j, \quad (2)$$

$$Nq_m - 2 \sum_{l \neq m}^M \varphi_{lm} = 2\pi J_m, \quad (3)$$

where $e^{i2\varphi_{lm}} = -(e^{iq_l + iq_m} + 1 - 2e^{iq_l})/(e^{iq_l + iq_m} + 1 - 2e^{iq_m})$ are the two-spinon scattering phases, the total spin momentum $P_s = \sum_m q_m$ is defined in the interval of $-\pi \dots \pi$, and N nonequal integers I_j and M nonequal integers J_m define the solution for the charge k_j and spin q_m (quasi)momenta of the N -particle state. This solution gives the eigenenergy of the many-body state as $E = t \sum_j k_j^2/2$ and its momentum as $P = \sum_j k_j$.

In the same limit, the eigenstates are factorized, $|\Psi\rangle = |\Psi_c\rangle \otimes |\Psi_s\rangle$, into a Slater determinant (such as for free particles) for the charge and a Bethe wave function (such as that for a Heisenberg chain) for the spin degrees of freedom [27,28],

$$|\Psi_c\rangle = \frac{1}{L^N} \sum_{Q,j} (-1)^Q \exp(iQ\mathbf{k} \cdot \mathbf{j}) a_{j_1}^\dagger \dots a_{j_N}^\dagger |0\rangle \quad (4)$$

$$|\Psi_s\rangle = \frac{1}{Z} \sum_{R, x_1 < \dots < x_M} \exp\left(i \sum_{l < m} \varphi_{R_l R_m} + iR\mathbf{q} \cdot \mathbf{x}\right) S_{x_1}^+ \dots S_{x_M}^+ |\downarrow\rangle, \quad (5)$$

where \mathbf{j} s are charge coordinates of N particles on the original Hubbard chain of length L , \mathbf{x} are positions of say M spins pointing up on the spin chain of N spins forming the spin part of the wave function, and the sums over Q and R run over all possible permutations of N momenta k_j and M momenta q_m , respectively. These wave functions are normalized to unity with the nontrivial normalization factor of the Bethe wave function being the determinant $Z^2 = \det \hat{Q}$ of an $M \times M$ matrix with the following diagonal $Q_{aa} = N - \sum_{l \neq a}^M 4(1 - \cos q_l)/(e^{iq_l} + e^{-iq_a} - 2)/(e^{iq_a} + e^{-iq_l} - 2)$ and off-diagonal $Q_{ab} = 4(1 - \cos q_b)/(e^{iq_a} + e^{-iq_b} - 2)/(e^{iq_b} + e^{-iq_a} - 2)$ with $a \neq b$ elements [29]. Here, the spinless Fermi a_j^\pm and the purely spin S_j^\pm operators can be recombined in the original electron operators $c_{j\alpha}^\dagger$ by introducing an insertion (deletion) of the spin-down state at a given position x in the spin chain operator $I_x(D_x)$ as $c_{j\uparrow}^\dagger = a_j^\dagger S_x^+ I_x$, $c_{j\downarrow}^\dagger = a_j^\dagger I_x$, $c_{j\uparrow} = a_j D_x S_x^-$, and $c_{j\downarrow} = a_j D_x S_x^- S_x^+$ [30].

The zero temperature Green's function is expressed in terms of the expectation values of the ladder operators as [31] $G_\alpha(k, E) = \sum_f [|\langle f | c_{k\alpha}^\dagger | 0 \rangle|^2 / (E - E_f + i\eta) + |\langle f | c_{k\alpha} | 0 \rangle|^2 / (E + E_f - i\eta)]$, where $c_{k\alpha}^\pm = \sum_j c_{j\alpha}^\pm e^{\pm ikj} / \sqrt{L}$ is the Fourier transform and η is an infinitesimally small real number. The factorization of the wave functions makes this calculation easier since the matrix elements become a product of two factors $\langle f | c_{j\alpha}^\pm | 0 \rangle = \langle f | c_{j\alpha}^\pm | 0 \rangle_c \langle f | c_{j\alpha}^\pm | 0 \rangle_s$, where $0 = (\mathbf{k}^0, \mathbf{q}^0)$ and $f = (\mathbf{k}^f, \mathbf{q}^f)$ are the momenta of the ground and excited states. The model in Eq. (1) has the symmetry of swapping the spin indices $\uparrow \leftrightarrow \downarrow$, which its Green's function also possesses $G_\uparrow(k, E) = G_\downarrow(k, E)$. Therefore, we will consider only $\alpha = \uparrow$. The charge part of the matrix element is an expectation value with respect to the state in Eq. (4) that evaluates as a N -fold sum over coordinates \mathbf{j} producing a determinant of the Vandermonde type. Then, application of the generalized Cauchy formula gives the following result for the annihilation operator $c_{j\uparrow}$ [32,33],

$$\langle f | c_{j\uparrow} | 0 \rangle_c = \frac{2^{N-1} \sin^{N-1} \left(\frac{P_s^f - P_s^0}{2} \right) e^{i(P_0 - P_f)j}}{L^{N-(1/2)}} \times \frac{\prod_{i < j}^{N-1} (k_i^f - k_j^f) \prod_{i < j}^N (k_i^0 - k_j^0)}{\prod_{i,j}^{N,N-1} (k_j^f - k_i^0)}, \quad (6)$$

where $\langle f | c_{j\uparrow} | 0 \rangle_c \equiv \langle \Psi_c^f | a_j | \Psi_c^f \rangle$ and the low-density limit in which $k_j^{0,f} \ll 1$ is already taken.

The spin part part of the matrix elements is an expectation value with respect to the states in Eq. (5) that is less straightforward to evaluate. A mathematical technique for dealing with these Bethe states analytically was invented in an algebraic form [34], leading to calculation of the correlation function for the noninteracting quantum magnets described by the Heisenberg model [35,36]. However, this result cannot be used here directly since the operators of the Hubbard model $c_{j\uparrow}^\pm$ change the length of the spin chain, making the constructions of Ref. [34] for the bra and ket states incompatible with each other. We resolve this problem by representing operators

of one algebra (for the longer chain) through the other (for the shorter chain) and the spin operators of the extra site. Then, explicit evaluation of the expectation value in the spin subspace of the additional site restores applicability of the methods in Ref. [23], and we obtain the spin part of the matrix element in terms of the determinant of a $M \times M$ matrix (see the details of this calculation in Ref. [27]),

$$\begin{aligned} \langle f | c_{j\uparrow} | 0 \rangle_s &= \frac{\det \hat{R}}{Z_0 Z_f} \prod_{i,j}^{M-1,M} \left(e^{iq_i^f} + e^{-iq_j^0} - 2 \right) \\ &\times \prod_{i \neq j}^{M-1} \left(e^{iq_i^f} + e^{-iq_j^f} - 2 \right)^{-\frac{1}{2}} \prod_{i \neq j}^M \left(e^{iq_i^0} + e^{-iq_j^0} - 2 \right)^{-\frac{1}{2}}, \end{aligned} \quad (7)$$

where $\langle f | c_{j\uparrow} | 0 \rangle_s \equiv \langle \Psi_s^f | D_x S^- | \Psi_s^0 \rangle$ and the elements of matrix \hat{R} are

$$R_{ab} = \frac{e^{iq_b^0(N-1)} \prod_{j \neq a}^{M-1} \left(-\frac{e^{iq_j^f + iq_b^0 + 1 - 2e^{iq_j^f}}}{e^{iq_j^f + iq_b^0 + 1 - 2e^{iq_b^0}}} \right) - 1}{(e^{-iq_a^f} - e^{-iq_b^0})(e^{iq_a^f} + e^{-iq_b^0} - 2)}, \quad (8)$$

$$R_{Mb} = \frac{e^{ik_b^0} \prod_{i \neq b}^M (e^{iq_i^0} + e^{-iq_b^0} - 2)}{\prod_j^{M-1} (e^{iq_i^f} + e^{-iq_b^0} - 2)} \quad (9)$$

for $a < M$ and for $a = M$, respectively. Together Eqs. (6)–(9) give the complete analytical expression for the matrix element for the 1D Hubbard model. Repeating the same calculation for the matrix element of the creation operator $\langle f | c_{k\uparrow}^\dagger | 0 \rangle$, we obtain the same expressions as in Eqs. (6)–(9) in which the momenta are swapped, $\mathbf{k}^0, \mathbf{q}^0 \leftrightarrow \mathbf{k}^f, \mathbf{q}^f$, and the particle (spin) quantum number is increased by one $N \rightarrow N + 1$ ($M \rightarrow M + 1$).

The response of a many-body system to a single-particle excitation at a given momentum and energy is described by the spectral function, making this observable particularly interesting for the experiments on spectroscopy. It is related to Green's function as $A_\alpha(k, E) = -\text{Im } G_\alpha(k, E) \text{sgn}(E - E_0)/\pi$ [31] giving

$$\begin{aligned} A_\alpha(k, E) &= \sum_f |\langle f | c_{k\alpha}^\dagger | 0 \rangle|^2 \delta(E - E_f + E_0) \\ &+ \sum_f |\langle f | c_{k\alpha} | 0 \rangle|^2 \delta(E + E_0 - E_f), \end{aligned} \quad (10)$$

where the sum over the result in Eqs. (6)–(9) [37] needs to be evaluated over exponentially many final states f . It can be performed based on emergence of the hierarchy of modes: Away from the low-energy regime around the Fermi points the many-body continuum splits itself into levels (consisting of a polynomial number of excitations on each of them) according to their spectral strength, which is proportional to integer powers of a small parameter $1/L^2$ [38].

In the presence of spin and charge degrees of freedom this phenomenon manifests itself on the microscopic level in the following way. For the ground states, the charge and spin momenta form two Fermi seas that correspond to se-

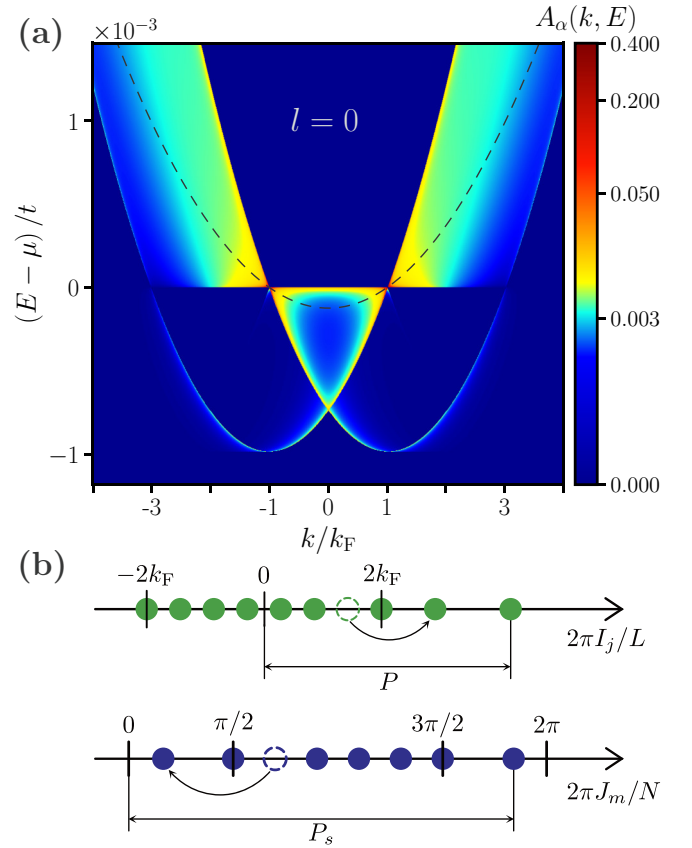


FIG. 2. (a) Spectral function $A_\alpha(k, E)$ of the model in Eq. (1) evaluated in the $U/t = \infty$ limit using Eqs. (6)–(10) for $N = 500$ particles where only the leading level of the hierarchy $l = 0$ was taken into account in the sum in Eq. (10). The single-particle dispersion of free particles $U/t = 0$ is superimposed as a dashed line. (b) Two sets of integer numbers, I_j for the charge and J_m for spin degrees of freedom, defining the Lieb-Wu equations (2) and (3) for an excited state with momentum P and the total spin momentum P_s ; two “electron-hole” pairs are shown as examples of lowering the level of the hierarchy, see the text. For a spin-unpolarized system, the number of spin degrees of freedom is $M = N/2$ that makes the charges’ density twice larger than that of the spins.

lecting the nonequal integer numbers in Eqs. (2) and (3) as $I_j = -N/2 \dots N/2$ and $J_m = -(N - M)/2 \dots (N + M)/2$ [26], see the illustration in Fig. 2(b). The charge part of the spectral amplitude for a generic excitation above this ground-state $|\langle f | c_{k\alpha}^\dagger | 0 \rangle_c|^2$ given by Eq. (6) is vanishingly small in the thermodynamic limit since it is proportional to $1/L^{2N}$. However, the factor $k_j^f - k_i^0$ in the denominator of Eq. (6) produces a singularity that is cut off by $1/L$ canceling a power of $1/L^2$ in the spectral amplitude each time a charge momentum of the excited state is equal to a momentum of the ground state. This property selects a specific set of the excitations for which a charge is added above the ground—see the charge state in Fig. 2(b)—and for which the $1/L^{2N}$ factors are canceled altogether making $|\langle f | c_{k\alpha}^\dagger | 0 \rangle_c|^2 \sim 1$. Adding each “electron-hole” pairs of charges on top of these states multiplies the spectral amplitude by an extra small parameter $1/L^2$ since some powers of the normalization factor $1/L^{2N}$ remain uncanceled.

For the spin part of the spectral amplitude $|\langle f|c_{k\alpha}^\dagger|0\rangle_s|^2$ given by Eq. (7), emergence of a small parameter is similar. The normalization factor $1/(Z_0 Z_f)$ makes the amplitude proportional to a vanishing in the thermodynamic limit factor $1/N^{2M}$ and the singularity $1/(e^{-iq_a^f} - e^{-iq_b^f})$ in the matrix elements in Eq. (8) cancels it altogether for a subset of states for which only one spin is added on top of the spin ground states—see the spin state in Fig. 2(b)—making $|\langle f|c_{k\alpha}^\dagger|0\rangle_s|^2 \sim 1$. Adding each “electron-hole” pair of spins on top multiplies the spectral amplitude by an extra small parameter $1/N^2$.

Combined, these two properties result in the hierarchy of modes for both types of the degrees of freedom with the spectral power for the strongest excitations being on the order of $|\langle f|c_{k\alpha}^\dagger|0\rangle|^2 \sim 1$ and the subleading excitations being weak as $|\langle f|c_{k\alpha}^\dagger|0\rangle|^2 \sim 1/(N^{2m}L^{2n})$, where $l = n + m > 0$ and n and m are the numbers of extra “electron-hole” pairs in the charge and spin Fermi seas, respectively. Close to the Fermi points this hierarchy of modes breaks down. The spectral amplitudes of all excitations become of the same order forming spin and charge-density waves, and the spinful TLL theory becomes a better approach for calculating correlation functions [5].

Analyzing first the nonlinear regime away from the Fermi points, we evaluate the spectral function in Eq. (10) numerically taking into account only the top level of the hierarchy $l = 0$ in the sum over f [39]. The result is presented in Fig. 2(a) where the Fermi momentum is defined by the free particle limit as $k_F = \pi N/2$ and the corresponding sum rule (which also includes the linear regime around the Fermi points) is already fulfilled as $2 \int_{-\infty}^{\infty} dk \int_{-\infty}^0 dE A(k, E)/N \simeq 61\%$ even for a large number of particles $N = 500$. Unlike the case of spinless fermions [38], the excitations at the top level of the hierarchy form a continuum for fermions with spin-1/2 since adding an electron with spin-1/2 adds simultaneously both charge and spin with two different momenta P and P_s , see Fig. 2(b). In this continuum, only two nonequivalent peaks emerge away from the Fermi points: One connects the $\pm k_F$ points and the other connects the $-k_F, 3k_F$ points (or equivalently, the $-3k_F, k_F$ points) on the $E = \mu$ line. Around the $\pm k_F$ Fermi points, these nonlinear peaks become two linear peaks that are the manifestation of the collective spin (i.e., spinon) and charge (i.e., holon) modes predicted by the spinful TLL model at low energy [4,5]. This identifies the nonlinear modes as being collective spin and charge excitations as well (see more details in Ref. [27]) and shows that the spin-charge separation still manifests itself in observables beyond the linear TLL limit.

The line shapes of the peaks away from the low-energy region have the form of divergent power laws, e.g., the particular momentum-dependent exponent was predicted for the spinon mode (which correspond to the spectral edge at finite U) in Refs. [15,40] and experimentally confirmed in Ref. [20]. The nonlinear holon and spinon modes were observed directly in the momentum-energy resolved magnetotunneling experiments in semiconductor quantum wires at intermediate coupling strength [19,22] that strongly suggests their robustness also for interactions with finite range and of finite strength, beyond the regime of the present calculation.

The momentum distribution function is another observable of interest in the many-body systems. It can be obtained from

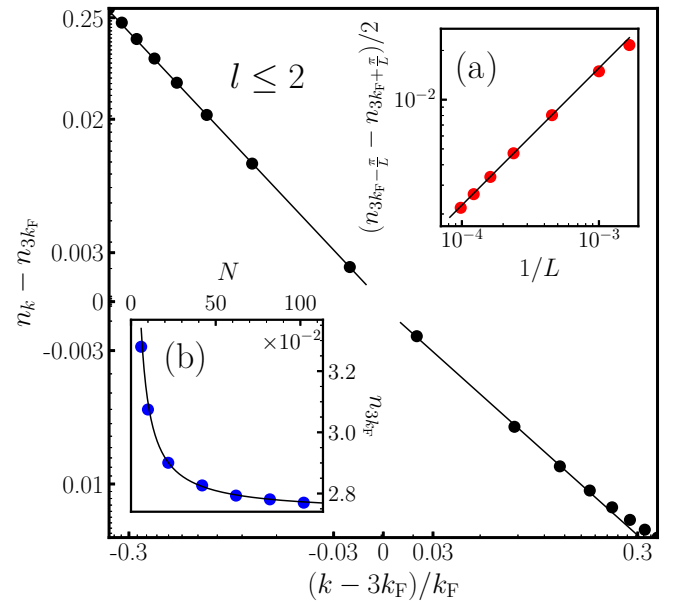


FIG. 3. Momentum distribution function n_k around $3k_F$ on the log-log scale for $N = 80$ particles where the three leading levels of the hierarchy of modes $l \leq 2$ were taken into account in the sum in Eq. (11). The dashed solid lines are power-law functions for $k < 3k_F$ and for $k > 3k_F$ giving the exponent as $a_{3k_F} = 0.787 \pm 0.067$ where the value is the average of the two and the error bars are the difference. Inset (a): Finite-size cutoff for n_k as the function of inverse system size $1/L$ on the log-log scale at $3k_F$. The solid line is a power-law fit giving $a_{3k_F} = 0.838$ within the accuracy of the fitting n_k directly. Inset (b): The value of n_k at $3k_F$ as a function of the particle number N . The solid line is a fit of finite-size corrections, $n_{3k_F} = C_{3k_F} + b/N$, giving $C_{3k_F} = 0.027$.

Green's function as $n_k = \int dE \Theta(E_0 - E) \text{Im} G_\alpha(k, E)/\pi$ [31] giving

$$n_k = \sum_f |\langle f|c_{k\alpha}|0\rangle|^2. \quad (11)$$

One of the regions of particular interest for this quantity is proximity of the Fermi point in which the infinite number the “electron-hole” pairs has to be included in the sum over f . This can be, at least, partially accounted for by adding subleading levels of the hierarchy. The result of the numerical calculation for $N = 200$ and $l \leq 1$ is presented in Fig. 1(a) where the sum rule already accounts for $2 \int dk n_k/N \simeq 86\%$ of the particles.

Singularities in n_k were introduced as the definition of a Fermi surface in many-body systems in the Luttinger theorem [41]. Here, we use this definition to interpret the result in Fig. 1. Due to the TLL physics, the singularity at k_F is weaker in 1D [42], e.g., instead of a discontinuity in n_k in $D > 1$ dimensions n_k is finite with a divergence appearing in dn_k/dk in 1D, see Fig. 1(b). Inspecting the result in Fig. 1(a), we find a second singularity of same order at $3k_F$, see Fig. 1(c). And we find no divergencies at any other points, e.g., see Fig. 1(d). The second singularity can be interpreted as a direct manifestation of spin-charge separation beyond the low-energy regime, which facilitates appearance of two Fermi points at different momenta since the density of nonlinear holons twice

larger than that of the nonlinear spinons in a spin-unpolarized system. Note that $n_{k=0} \simeq 0.7$ in Fig. 1(a) is still smaller than $n_{k=0} = 1$ for the free system so $\sim 30\%$ of particles is redistributed above k_F providing a significant amplitude around the $3k_F$ point.

The coinciding order of both singularities suggests that the states around $3k_F$ are also described by a TLL model, which predicts a power-law behavior of the momentum distribution function [1],

$$n_k = C_{(3)k_F} + \dots \text{sgn}[(3)k_F - k] |k - (3)k_F|^{\alpha_{(3)k_F}}, \quad (12)$$

where $\alpha_{(3)k_F}$ is a real exponent and $C_{(3)k_F}$ is the value of n_k exactly at $(3)k_F$. Fitting a linear function on a log-log plot of n_k extracts the exponent around $3k_F$ directly, see Fig. 3. Alternatively, the same exponent can be extracted from the finite-size cutoff at $3k_F$, see inset (a) in Fig. 3. Both methods give $a_{3k_F} = 0.787 \pm 0.067$. The scaling of n_{3k_F} with the system size gives a finite amplitude in the thermodynamic limit $C_{3k_F} = 0.027$, see inset (b) in Fig. 3. In all of these numerical calculations the number of the levels l used in calculating Eq. (11) was increased until the next subleading level was

giving only a small correction to the value of n_k at each point. Application of the same procedure around k_F gives $C_{k_F} = 0.477$ and $\alpha_{k_F} = 0.124 \pm 0.020$ [27], which is the well-known result of the TLL theory $\alpha_{k_F} = 0.125$ [43–45]. However, only one attempt of using the TLL approach at $3k_F$ was made in Ref. [46] in which $a_{3k_F} = 1.125$ was obtained, suggesting a lower order (in $d^2 n_k / dk^2$) of the second singularity. This discrepancy can be attributed to using both spinon and holon modes in Ref. [46], whereas the present microscopic calculation shows in Fig. 2(a) that only the holon modes can form a TLL at $3k_F$. In conclusions, we have shown that spin-charge separation can split one Fermi surface into two. Together with the recent experimental observation of spin-charge splitting of the whole band in Ref. [22], it demonstrates that this phenomenon is more general than it was originally anticipated, and that substantial features of the Fermi gas still survive in 1D despite formation of a genuine many-body continuum by the interactions.

I thank A. Schofield for discussions and helpful comments. This work was funded by the Deutsche Forschungsgemeinschaft (DFG) via Project No. 461313466.

-
- [1] T. Giamarchi, *Quantum Physics in One Dimension* (Clarendon, Oxford, 2003).
 - [2] S. Tomonaga, *Prog. Theor. Phys.* **5**, 544 (1950).
 - [3] J. M. Luttinger, *J. Math. Phys.* **4**, 1154 (1963).
 - [4] F. D. M. Haldane, *J. Phys. C: Solid State Phys.* **14**, 2585 (1981); J. Voit, *Phys. Rev. B* **47**, 6740 (1993).
 - [5] V. Meden and K. Schönhammer, *Phys. Rev. B* **46**, 15753 (1992).
 - [6] O. M. Auslaender, H. Steinberg, A. Yacoby, Y. Tserkovnyak, B. I. Halperin, K. W. Baldwin, L. N. Pfeiffer, and K. W. West, *Science* **308**, 88 (2005).
 - [7] Y. Jompol, C. J. B. Ford, J. P. Griffiths, I. Farrer, G. A. C. Jones, D. Anderson, D. A. Ritchie, T. W. Silk, and A. J. Schofield, *Science* **325**, 597 (2009).
 - [8] R. Claessen, M. Sing, U. Schwingenschlögl, P. Blaha, M. Dressel, and C. S. Jacobsen, *Phys. Rev. Lett.* **88**, 096402 (2002).
 - [9] B. J. Kim, H. Koh, E. Rotenberg, S.-J. Oh, H. Eisaki, N. Motoyama, S. Uchida, T. Tohyama, S. Maekawa, Z.-X. Shen, and C. Kim, *Nat. Phys.* **2**, 397 (2006).
 - [10] J. Vijayan, P. Sompet, G. Salomon, J. Koepsell, S. Hirthe, A. Bohrdt, F. Grusdt, I. Bloch, and C. Gross, *Science* **367**, 186 (2020).
 - [11] K. V. Samokhin, *J. Phys.: Condens. Matter* **10**, L533 (1998).
 - [12] T. Karzig, L. I. Glazman, and F. von Oppen, *Phys. Rev. Lett.* **105**, 226407 (2010).
 - [13] A. Levchenko and T. Micklitz, *J. Exp. Theor. Phys.* **132**, 675 (2021).
 - [14] Z. Ristivojevic and K. A. Matveev, *Phys. Rev. Lett.* **127**, 086803 (2021).
 - [15] A. Imambekov and L. I. Glazman, *Phys. Rev. Lett.* **102**, 126405 (2009).
 - [16] T. L. Schmidt, A. Imambekov, and L. I. Glazman, *Phys. Rev. Lett.* **104**, 116403 (2010).
 - [17] A. Imambekov, T. L. Schmidt, and L. I. Glazman, *Rev. Mod. Phys.* **84**, 1253 (2012).
 - [18] G. Barak, H. Steinberg, L. N. Pfeiffer, K. W. West, L. Glazman, F. von Oppen, and A. Yacoby, *Nat. Phys.* **6**, 489 (2010).
 - [19] M. Moreno, C. J. B. Ford, Y. Jin, J. P. Griffiths, I. Farrer, G. A. C. Jones, D. A. Ritchie, O. Tsyplatyev, and A. J. Schofield, *Nat. Commun.* **7**, 12784 (2016).
 - [20] Y. Jin, O. Tsyplatyev, M. Moreno, A. Anthore, W. Tan, J. Griffiths, I. Farrer, D. Ritchie, L. Glazman, A. Schofield, and C. Ford, *Nat. Commun.* **10**, 2821 (2019).
 - [21] S. Wang, S. Zhao, Z. Shi, F. Wu, Z. Zhao, L. Jiang, K. Watanabe, T. Taniguchi, A. Zettl, C. Zhou, and F. Wang, *Nature Mater.* **19**, 986 (2020).
 - [22] P. M. T. Vianez, Y. Jin, M. Moreno, A. S. Anirban, A. Anthore, W. K. Tan, J. P. Griffiths, I. Farrer, D. A. Ritchie, A. J. Schofield, O. Tsyplatyev, and C. J. B. Ford, [arXiv:2102.05584](https://arxiv.org/abs/2102.05584).
 - [23] V. E. Korepin, N. M. Bogoliubov, and A. G. Izergin, *Quantum Inverse Scattering Methods and Correlation Functions* (Cambridge University Press, Cambridge, UK, 1993).
 - [24] The definition of a Fermi point (or surface) for a many-body system as a special point in n_k was given by Luttinger and Haldane [41,42].
 - [25] This limit corresponds to the continuum model with a finite mass and a δ -functional density-density interaction in which mass m is inversely proportional to the hopping amplitude t , the interaction strength is proportional to U , and the lattice parameter only plays the role of an ultraviolet cutoff.
 - [26] E. H. Lieb and F. Y. Wu, *Phys. Rev. Lett.* **20**, 1445 (1968).
 - [27] See Supplemental Material at <http://link.aps.org/supplemental/10.1103/PhysRevB.105.L121112> for details, which includes Refs. [47–54].
 - [28] M. Ogata and H. Shiba, *Phys. Rev. B* **41**, 2326 (1990).
 - [29] M. Gaudin, B. M. McCoy, and T. T. Wu, *Phys. Rev. D* **23**, 417 (1981).
 - [30] Although the a_j^\pm and S_x^\pm operators obey the regular Fermi and spin commutation rules, the insertion (deletion) operator I_x (D_x)

- does not. In general, they also do not commute with the spin operators.
- [31] G. D. Mahan, *Many-Particle Physics* (Plenum, New York, 1990).
 - [32] K. Penc, K. Hallberg, F. Mila, and H. Shiba, *Phys. Rev. Lett.* **77**, 1390 (1996); *Phys. Rev. B* **55**, 15475 (1997).
 - [33] K. Penc and M. Serhan, *Phys. Rev. B* **56**, 6555 (1997).
 - [34] E. K. Sklyanin, L. A. Takhtajan, and L. D. Faddeev, *Theor. Math. Phys.* **40**, 688 (1979).
 - [35] N. Kitanine, J. Maillet, and V. Tetas, *Nucl. Phys. B* **554**, 647 (1999); N. Kitanine and J. M. Maillet, *ibid.* **567**, 554 (2000).
 - [36] J.-S. Caux and J. M. Maillet, *Phys. Rev. Lett.* **95**, 077201 (2005).
 - [37] Owing to the translational invariance of the model in Eq. (1) the expectation values of the c_k^\pm operator is related to the result in Eqs. (6)–(9) in a trivial way, $\langle f | c_{k\alpha}^\pm | 0 \rangle = \sqrt{L} \langle f | c_{l\alpha}^\pm | 0 \rangle \delta(k \mp P_f)$.
 - [38] O. Tsypliyatyev, A. J. Schofield, Y. Jin, M. Moreno, W. K. Tan, C. J. B. Ford, J. P. Griffiths, I. Farrer, G. A. C. Jones, and D. A. Ritchie, *Phys. Rev. Lett.* **114**, 196401 (2015); O. Tsypliyatyev, A. J. Schofield, Y. Jin, M. Moreno, W. K. Tan, A. S. Anirban, C. J. B. Ford, J. P. Griffiths, I. Farrer, G. A. C. Jones, and D. A. Ritchie, *Phys. Rev. B* **93**, 075147 (2016).
 - [39] Addition of extra excitations with $l > 0$ to the spectral function in Eq. (10) produces extra levels of the hierarchy beyond the low-energy limit that correspond to mirroring with respect to the $E = \mu$ line and translating by integer multiples of $2k_F$ and $4k_F$ the continuum picture of the top level $l = 0$ in Fig. 2. However, the overall amplitude of these replicas is proportional to positive integer powers of the small parameters $1/L^2$ and $1/N^2$.
 - [40] O. Tsypliyatyev and A. J. Schofield, *Phys. Rev. B* **90**, 014309 (2014).
 - [41] J. M. Luttinger, *Phys. Rev.* **119**, 1153 (1960).
 - [42] F. D. M. Haldane, in *Proceedings of the International School of Physics “Enrico Fermi,” Course CXXI: “Perspectives in Many-Particle Physics,”* edited by R. Broglia and J. R. Schrieffer (North Holland, Amsterdam, 1994), pp. 5–30.
 - [43] H. J. Schulz, *Phys. Rev. Lett.* **64**, 2831 (1990).
 - [44] H. Frahm and V. E. Korepin, *Phys. Rev. B* **42**, 10553 (1990).
 - [45] N. Kawakami and S.-K. Yang, *Phys. Lett. A* **148**, 359 (1990).
 - [46] K. Penc and J. Sólyom, *Phys. Rev. B* **44**, 12690 (1991).
 - [47] H. Bethe, *Z. Phys.* **71**, 205 (1931).
 - [48] M. Gaudin, *Phys. Lett. A* **24**, 55 (1967).
 - [49] C. N. Yang, *Phys. Rev. Lett.* **19**, 1312 (1967).
 - [50] M. Gaudin, *The Bethe Wavefunction* (Cambridge University Press, Cambridge, UK, 2014).
 - [51] F. H. L. Essler, H. Frahm, F. Göhmann, A. Klümper, and V. E. Korepin, *The One-Dimensional Hubbard Model* (Cambridge University Press, Cambridge, UK, 2005).
 - [52] N. A. Slavnov, *Theor. Math. Phys.* **79**, 502 (1989).
 - [53] V. E. Korepin, *Commun. Math. Phys.* **86**, 391 (1982).
 - [54] V. G. Drinfeld, *Sov. Math. Dokl.* **28**, 667 (1983).